Sensors and Actuators A 203 (2013) 142–148

Contents lists available at ScienceDirect

Sensors and Actuators A: Physical

journal homepage: www.elsevier.com/locate/sna

Design and analysis of functional multiwalled carbon nanotubes for infrared sensors

R. Afrin [a], N.A. Shah [a,*], M. Abbas [a], M. Amin [a], A.S. Bhatti [b]

[a] Thin Film Technology Laboratory, Department of Physics, COMSATS Institute of Information Technology, Islamabad 44000, Pakistan
[b] Centre for Micro & Nano Devices, Department of Physics, CIIT, Islamabad, Pakistan

ARTICLE INFO

Article history:
Received 14 May 2013
Received in revised form 7 August 2013
Accepted 12 August 2013
Available online 6 September 2013

Keywords:
Carbon nanotubes
Scanning electron microscopy
Infrared sensors

ABSTRACT

In this paper, we report the comparison of infrared detection based on buckypapers of chemically modified multiwalled carbon nanotubes by carboxyl and thiol groups. We observed that functionalized carbon nanotube buckypapers had a significant impact on radiation sensing at room temperature. Nanotubes buckypapers were formed by successively increasing cross-linker reagent in carbon nanotubes. It was observed that infrared sensitivity of resistively read-out of carboxylated and thiolated buckypapers increased by increasing the cross-linker reagent up to certain limit. Further increase in cross-linker reagent results in brittleness of buckypaper. The maximum sensitivity of carboxylated and thiolated buckypapers was 3.4% and 16.07% while minimum response time of carboxylated and thiolated buckypapers was 1.29 s and 6.09 s, respectively. X-ray diffraction, scanning electron microscopy, transmission electron microscopy, Raman spectroscopy and Fourier transform infrared spectroscopy were used for analysis of presences of nanotubes, structural morphology and defect density to evaluate all the modifications of the nanotubes structure and the nature of the compounds added to the nanotubes surface by functionalization treatment.

1. Introduction

Carbon nanotubes (CNTs) have been known as the exceptionally promising material for infrared (IR) sensors. One dimensional quantum nature and large surface to volume ratio of CNTs makes their intrinsic properties highly sensitive to small external perturbations [1–7]. Infrared photodectors are highly desirable for various applications including remote sensing and biological imaging [8]. Multiwalled carbon nanotubes (MWCNTs) based infrared detectors have received much attention due to their moderate band gap of 0.4–6.0 eV and high absorption efficiency in IR band [9]. The extremely small specific heat of a carbon nanotube gives a bolometric (change in resistance under heating) thermal detector with a very fast response time and good sensitivity [10–12].

CNTs infrared detectors were developed based on thermal and photo effects. In thermal effect like Bolometers, the output signal (resistance, current or voltage) was produced by temperature change due to infrared illumination [13–15]. Moreover in photo detector electron–hole pairs are generated and dissociated by photon absorption of nanotubes leading the photo current or photo voltage in the device [16]. Bolometer devices were fabricated using single or multiple tube arrays of single-walled and multiwalled carbon nanotubes in the form of pristine or composites as active material for infrared detection [15,17–21]. For instance, the Mikhail et al. reported the photo response of suspended SWCNTs network under vacuum on infrared illumination. The results showed the Bolometric effect due to ultrafast relaxation of photo excited carriers under IR illumination and transferring radiation energy to crystal lattice which leads to change in resistance by rising the temperature of samples [13]. Gohier et al. reported the Bolometric effect using MWCNTs deposited on flexible polyimide substrate. The response to IR radiation had a significant resistance drop of 0.35% after 10 s of illumination at room temperature [9].

Regardless of these remarkable results, scientists are still trying to improve the integrity, detectivity, responsivity, and signal to noise ratio of the CNTs-based Bolometers. Alternatively, buckypapers of CNTs have provided a potential approach to enhance the integrity and sensitivity of infrared sensors [22].

CNTs with no intrinsic defects are chemically inert due to sp^2 hybridization in C—C bonding. Defects were created by acid treatment which causes the functional group to attach on defect sites along side walls of nanotubes [23–25]. The functional groups induces the localized impurity states near the Fermi level within the band gap region along the radial directions on the side walls of nanotubes and forms the local sp^3 rehybridization of C—C bonding [26]. These impurity states dislocates the conducting π and π^*

* Corresponding author. Tel.: +92 3215105363; fax: +92 514442805.
E-mail addresses: raheen_06@yahoo.com (R. Afrin), nabbasqureshi@yahoo.com, nazar_abbas@comsats.edu.pk (N.A. Shah), manzar@comsats.edu.pk (M. Abbas), aminislamabad@yahoo.com (M. Amin).

0924-4247/$ – see front matter © 2013 Elsevier B.V. All rights reserved.
http://dx.doi.org/10.1016/j.sna.2013.08.018

states. The scattering centers were formed due to functionalization which disturbs the ballistic conducting properties of nanotubes and leads the considerable change in electronic states as well as in the electrical properties of nanotubes [27]. Furthermore, the electrodes on the outermost shells of MWCNTs, which may be either semiconducting or metallic, plays the dominant role in electrical transport via photon absorption which causes the phonons generation and exciton dissociation in nanotubes [12]. The semiconductor band gap of MWCNTs decreases inversely with the tube diameter making nanotubes the excellent candidate for infrared sensing. Motivated by these advantages, we have investigated the infrared photoresponse of unsuspended buckypapers of nanotubes.

In this work, buckypapers of chemically side-wall surface modified semiconducting CNTs by attaching different functional groups: carboxylic acid (—COOH) and thiol (—SH) were utilized as an important step for sensing infrared radiations. Buckypapers of functionalized CNTs were obtained by covalent cross-linking of nanotubes. The cross-linking between multiwall nanotubes was achieved by controlled chemical treatments which enhances the mechanical strength as well as to characterize the electrical conduction behavior as compared to those which are linked by only weak interactions. Vacuum filtration process was used for buckypaper formation which provides the control of homogeneous thickness of buckypaper. The density and thickness of buckypaper has been maintained by observing the same weight measurements in each chemical reaction of reactants. The CNTs in random network have been interconnected through electrodes for continuous electrical paths between electrodes. It revealed the nonlinear current–voltage behavior and showed the semiconducting transport in network. As functionalized CNTs produces the outer wall defects in nanotubes, so the incident radiation on buckypaper absorb energy and excitations and relaxation of valance electrons occurred with the creation of vibrational modes when the frequency of infrared was same as the vibrational frequency of attached bonds. This led to increase in thermal energy with electronic excitations and relaxation and hence the sensitivity via resistance change was observed which may be due to the charge carrier density.

The products were characterized by using X-ray powder diffraction (XRD, X'Pert PRO Difractometer, PANalytical) with Cu Kα radiation (λ = 1.5418 Å) and Fourier transform infrared (FT-IR) spectrophotometer Nexus 670 Thermo Nicolet in a Potassium Bromide (KBr) tablet. Field emission scanning electron microscopy (FESEM) images were taken on JSM JEOL 7401 with ultra high resolution at 3 kV. Transmission electron microscopy (TEM) images were taken on a JEOL, JEM-2010 microscope (200 kV) with EDX attachment. Raman spectroscopy of samples was taken on Lab RAM HR800. Electrical measurements were taken using optical microscope unit FS-70Z with keithley source meter model 2636A using two-probe method. Sensor measurements were made using keithley 6½ digital multimeter 2100.

2. Experimental

2.1. Chemicals

2-Mercaptoethanol ($HSCH_2CH_2OH$) 99% pure 4,4′-diaminobenzophenone ($C_{13}H_{12}N_2O$), nitric acid (HNO_3), hydrogen per oxide (H_2O_2), dimethylformamide (DMF) 99% pure, and all organic solvents were purchased from Sigma Aldrich and were used as received without further purification.

2.2. Fabrication and sensor setup

MWCNTs were purchased from Beijing DK Nano technology, China. The diameter of MWCNTs used was about 25–60 nm and length was 10–20 μm. The MWCNTs were purified by reflux and sonication in concentrated hydrochloric acid for 3 h at 30 °C followed by washing (pH 7), filtration and drying at 120 °C for 24 h in oven to remove the metal particles. For carboxylation, 0.5 g purified CNTs were mixed in 5 M HNO_3 and 35% H_2O_2 refluxed and sonicated for 5 h at 100 °C followed by washing (pH 7) with distilled water, filtration from suspension and drying at 120 °C in oven for 24 h. By this method, the obtained CNTs were oxidized by grafting COOH groups along the side walls of nanotubes and designated as MWCNTs–COOH. For thiolation of nanotubes, 0.02 g of carboxylated CNTs were dispersed in 50 mL methanol and sonicated for 30 min to form a stable black suspension. The suspension was added to solution of 2-mercaptoethanol (15 mL) and methanol (30 mL) and so obtained solution was sonicated for 3 h at room temperature. The 2-mercaptoethanol modified MWCNTs were achieved and denoted as MWCNTs–SH (Fig. 1a). The MWCNTs–SH were separated from the solution by centrifugation and dispersed in 50 mL ethanol then dried in oven at 120 °C for 24 h.

For the cross-linking or mat/buckypaper formation of nanotubes, 0.02 g of functionalized CNTs (—COOH, —SH) were dispersed in 15 mL dimethylformamide (DMF) by sonication for 30 min to obtain nanotube suspension. In a separate reaction container, 0.1 g of 4,4′-diaminobenzophenone was dissolved in 10 mL DMF. While stirring the CNTs, the 4,4′-diaminobenzophenone solution was injected at a rate of 0.1 mL/min into suspension. After the addition of 4,4′-diaminobenzophenone, the reaction mixture was allowed to stir for 12 h at 75 °C. The solution was then vacuum filtered (Nylon filtration membrane of 0.45 μm pore size) and dried at 120 °C for 24 h. The obtained buckypapers were designated as CNTCBPs and CNTTBPs for carboxylated and thiolated nanotubes respectively. The 4,4′-diaminobenzophenone was used as cross-linking agent between nanotubes (Fig. 1b) in order to form the buckypaper. In buckypaper formation the ratio of CNTs to cross-linker was 1:5, 1:7, 1:9 and 1:11 by weight. - Fig. 1c showed the experimental setup for measuring the sensing behavior. A MWCNTs cross-linked buckypaper and buckypaper on glass substrate with connecting wires is shown in Fig. 1d. Actual image of IR sensing setup and inset showing the sensor with holder are shown in Fig. 1e. The glass substrate was used as a mechanical support. The gold (Au) of 200 nm thickness was deposited through sputtering technique on glass substrate to make good contacts. The area of one electrode on glass substrate was 5 mm × 5 mm while the separation between the electrodes was a single line drawn by paper cutter on the deposited thin film for the formation of separate electrodes. The area of CNTs film was about 2 mm × 5 mm on gold electrodes. The unsuspended CNTs film was made by sonication the nanotubes in organic solvent for 15 min and suspension drop was placed between electrodes. Furthermore, the gold coated electrodes were connected through copper pressure contacts with resistance measuring device (Keithley 6½ digital multimeter 2100) and graphical read-out display unit. The buckypaper having area of 2 mm × 5 mm was placed on the glass substrate and the copper pressure contacts were directly made on buckypaper for onward connection to resistance measuring device. The electrical properties were measured using KI–tools application software of keithley multimeter. The infrared lamp (100 W) was used to bring out continuous infrared light for characteristic behavior. The wavelength of the infrared lamp was in far infrared range (50–1000 μm). All the measurements were performed in open air at room temperature.

3. Results and discussion

Fig. 2 shows the X-ray diffraction analysis of pristine carbon nanotubes. The XRD patterns were recorded in angle range (2θ) 20°–80°, where the angle 2θ is between the incident and scattered

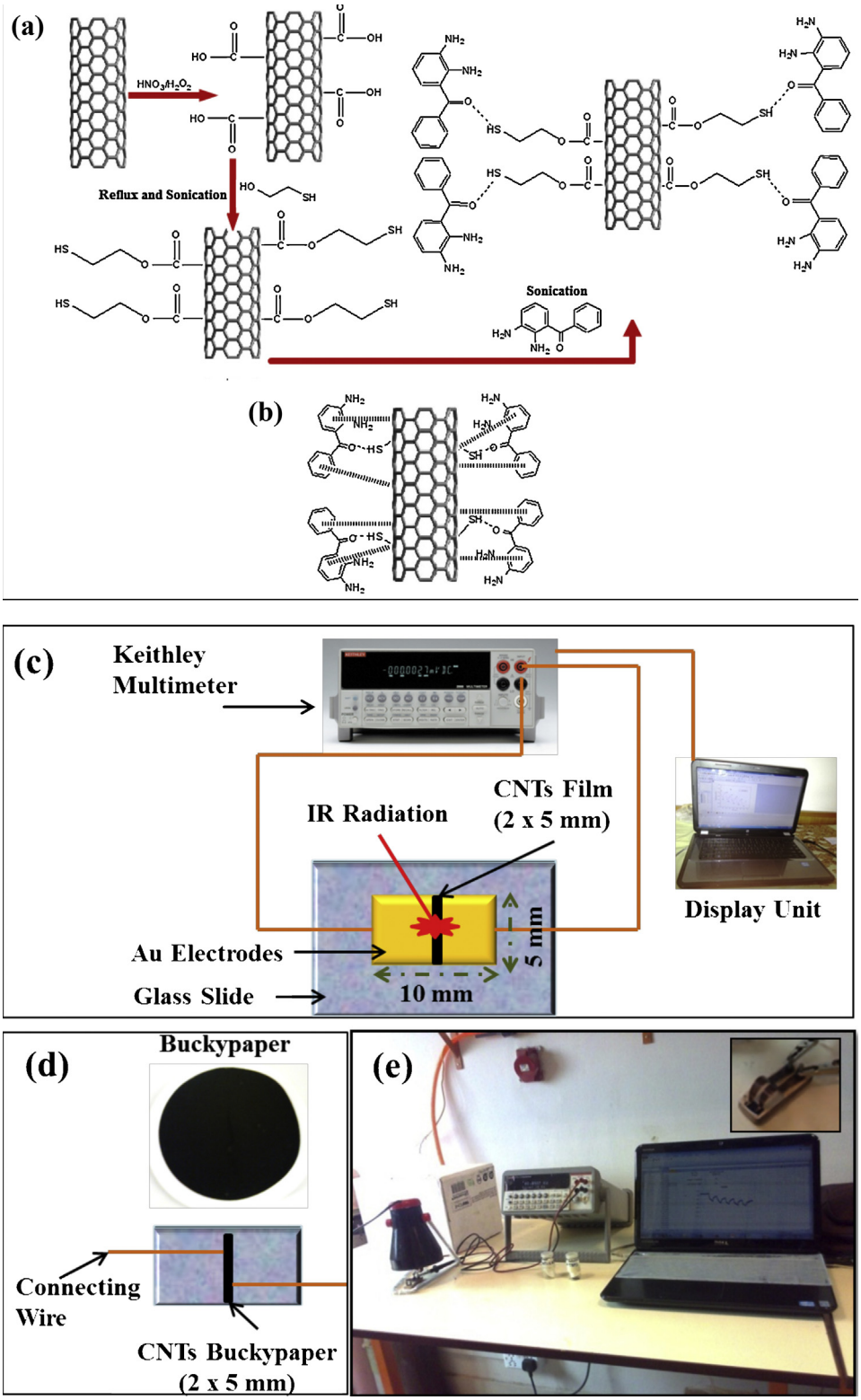

Fig. 1. (a) Reaction scheme for functionalization and cross-linking of MWCNTs; (b) $\pi-\pi$ stacking scheme; (c) schematic diagram of IR sensor setup; (d) a MWCNTs cross-linked buckypaper and buckypaper on glass substrate with connecting wires; (e) actual image of IR sensing setup and inset showing sensor with holder.

beams. The XRD pattern of CNTs samples revealed the presences of three peaks at 26.1576°, 44.3053° and 51.6300° corresponding to d_{002}, d_{101} and d_{102} reflections of hexagonal graphite structure of carbon atoms. The structure has p63/mmc space group with lattice constant $a = b = 2.47$ Å and $c = 6.8$ Å. The metal catalyst particles peaks at $2\theta = 21.8162°$, 36.0105° and 43.2058° were also observed.

The chemical bonding status of functionalized nanotubes was characterized by FT-IR spectroscopy as shown in Fig. 3. After acidic treatment, the CNTCBP showed the peak at 1360 cm^{-1} assigned to

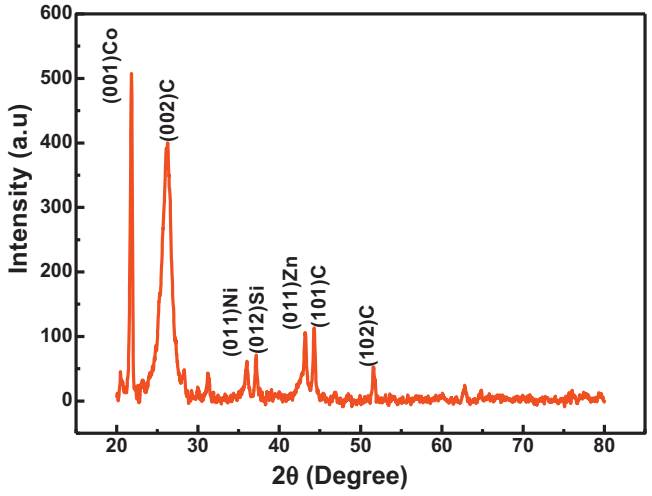

Fig. 2. XRD pattern of MWCNTs showing the catalyst particles and MWCNTs as graphitic carbon.

O—H bending vibrations in plane. The aromatic C=C stretching peak was observed at 1520 cm^{-1}.

The absorption peak at 1725 cm^{-1} corresponds to C=O was attributed to stretching vibrations of carboxylic acid groups (—COOH). The peaks at 2910 cm^{-1}, 2840 cm^{-1} and 2850 cm^{-1} corresponds to C—H stretching in both spectra, may be attributed due to the cross-linking of nanotubes. In CNTTBP, the bands in the range 1050–1200 cm^{-1} assigned to C=S were attributed to the stretching of thiocarbonyl groups [28]. The peaks at 785 cm^{-1} and 2345 cm^{-1} assigned to S—H were attributed to stretching vibrations of thiol groups. The broad asymmetrical stretching bands observed at around 3410 cm^{-1} in CNTCBP and 3390 cm^{-1} in CNTTBP spectra were assigned to O—H stretching bands and might be attributed to the trace of water in the KBr pellet used for analysis [29]. Fig. 4 showed the SEM micrograph of functionalized multiwall carbon nanotubes.

In Fig. 4a, we observed that MWCNT–COOH were obtained without shortening of CNTs and inset showed the pristine nanotubes which were purified by concentrated hydrochloric acid to remove the amorphous carbon and metal particles. Fig. 4b shows the CNTCBP buckypaper of oxidized nanotubes. These nanotubes were cross-linked through side walls via 4,4′-diaminobenzophenone which increases mechanical strength. Fig. 4c shows the thiol functionalized MWCNTs. The buckypaper of MWCNT–SH (Fig. 4d) was obtained by crossed linked via chemical reaction and observed stacking morphology which may

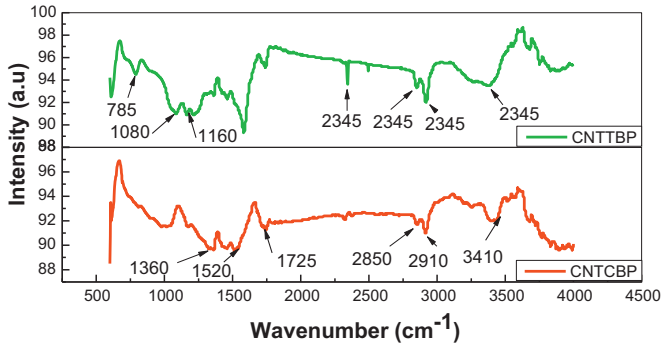

Fig. 3. FT-IR spectra of carboxylic acid attached buckypaper and thiolated buckypaper of multiwall carbon nanotubes.

be due to cross linking and more interactions between thiol groups.

The transmission electron microscopy (Fig. 5) visualizes the number of walls and linking of nanotubes to each other. Fig. 5a shows the buckypaper of carboxylated functionalized nanotubes, inset showed the magnified image of single CNT with outer wall defects. Fig. 5b shows the buckypaper of thiolated CNTs with outer wall defects (brown arrow) and surface linkage of nanotubes (yellow arrow).

The current–voltage plots for multiwall carbon nanotubes characterized by IV-system are shown in Fig. 6. The curves showed the semimetallic behavior. This semimetallic behavior might be due to the presence of semiconductive tubes and metallic tubes at the same time and amorphous carbon component was probably present [30,31]. *I–V* curve for CNTCOOH was nearly linear and average resistance was 0.5 kΩ while *I–V* curves for CNTCBPs and CNTTBPs showed the nonlinear behavior having average resistances of 1.6 kΩ and 3.1 kΩ, respectively. The observed nonlinear behavior suggests that the nanotubes buckypaper behaves as a semiconducting material after functionalization. *I–V* results were optimized for four samples for each type of CNTs.

The effect of different surface modifications on the chemical states of MWCNTs surface was investigated by Raman spectroscopy at 633 nm excitation wavelength. The bands of the Raman spectra for chemically modified MWCNTs are shown in Fig. 7. The main features in the Raman spectra are the fundamental vibrational excitations induced by different types of translational breaking symmetry perturbations attributed as D and G bands [32]. The disorder-induced D band around 1330 cm^{-1} corresponds to probe all phonon branches of graphite near the Γ and *K* points of the graphite two-dimensional (2D) brillouin zone due to surface defects bonding states on nanotubes. The tangential mode G at 1590 cm^{-1} which involves the optical phonon modes between two dissimilar carbon atoms in the unit cell corresponds to Raman enhanced C—C bonding oscillation inside the well crystallized graphite phase structures of MWCNTs. After chemical modification, the noticeable change consisting of increase in intensity of D-band relative to G band was found in the Raman spectra. This was because of covalently functionalized side walls altered to a more disordered structure due to thiolation and carboxylation. The intensity of Raman peaks I_D and I_G were determined and ratios of I_D/I_G can be characterized inversely proportional to the crystallinity L_a of conventional MWCNTs [32,33]. The calculated I_D/I_G ratios of CNTTBP, CNTCBP and CNTCOOH were 1.28, 1.22, and 1.20, respectively. The high I_D/I_G ratio indicates that there were more surface defects due to surface functional groups on MWCNTs after modifications. The intensity ratio of CNTCOOH was less than the intensity ratio of CNTCBP which showed that more defects were created along side walls due to cross-linking of nanotubes. The intensity ratio of CNTTBP showed more defects creation along side walls due to —SH covalent bonding and cross-linking of the nanotubes.

Fig. 8 compares the photo response in terms of resistance change of multiwall carbon nanotubes buckypapers. The change in resistance was caused by infrared radiation and given as $\Delta R = R - R_0$, Where 'R_0' is the sample resistance before infrared radiation turned on and '*R*' is the maximum resistance at infrared radiations. The sensitivity of sensor was measured by calculating mean values using $\Delta R/R_0$ for each cycle [15]. The observed response was due to presence of photo excited electrons and holes and also due to the rise in temperature [34]. Because the metal electrodes on the outermost shells of the MWCNTs either semiconducting or metallic play the dominant role in electrical transport via photons absorption which causes the phonons generation and exciton dissociation in the nanotubes.

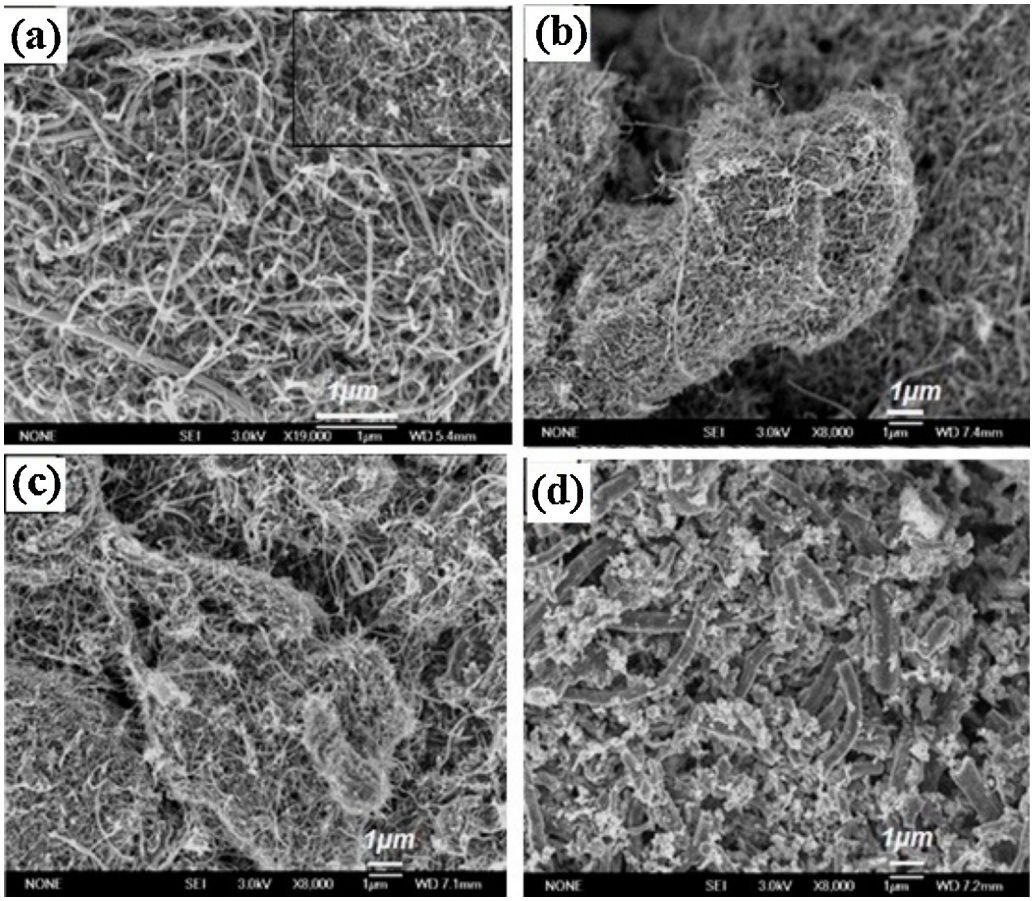

Fig. 4. SEM images of (a) MWCNT–COOH, (b) buckypaper of MWCNT–COOH, (c) MWCNT–SH, and (d) buckypaper of MWCNT–SH. Scale bars are in micrometers.

As the buckypaper of functionalized nanotubes was formed by chemically treating the nanotubes with 4,4′-diaminobenzophenon which increased mechanical strength and decreases electron transport. Since nanotubes were randomly distributed within the buckypaper and tube-end to body-end cross-linking most favorable which slow down the motion of electrons within the nanotubes due to creation of many defects along the side walls. Also chemical treatment can led to the p-doping which down shifts the Fermi level in the valance band and may results in weakening of all interband transitions in semiconducting tubes causing increase in resistance. This increase in resistance was observed via infrared sensing of device. During infrared illumination, the dangling bonds created by functional groups also absorb the infrared radiations along with the excitation of electrons and produces lattice vibrations resulting, more change in resistance thus increasing the sensitivity of the device. Different prototypes of each buckypaper were fabricated and optimized for infrared sensing as shown in Fig. 8. In this figure, the ratio of CNTs to cross-linker in buckypaper from bottom to top was 1:5, 1:7, 1:9 and 1:11 by weight. The sensitivity (R_s) of carboxylated nanotubes (Fig. 8a – CNTCOOH) thin film was 0.36% and response time (t_{res}) was 1.29 s. While the sensitivity of resistively read-out

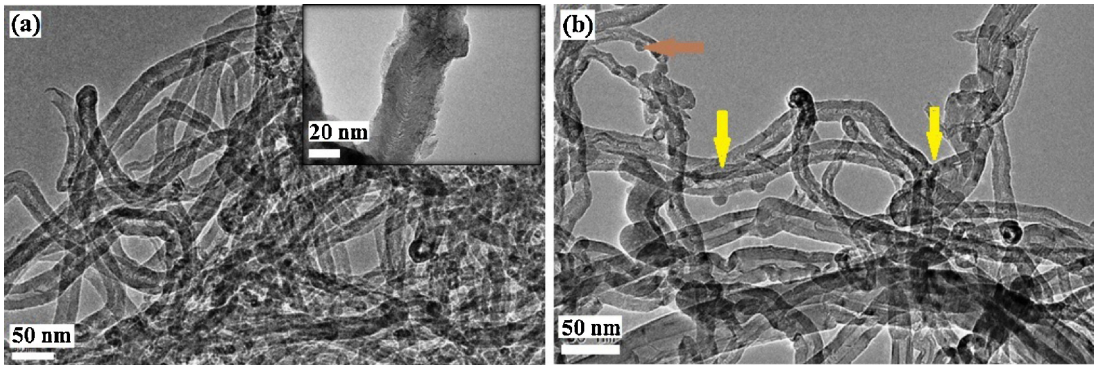

Fig. 5. (a) TEM image of MWCNT–COOH buckypaper inset shows the magnified image of single CNT with outer wall defects (b) TEM image of MWCNT–SH buckypaper. Brown arrow shows the defects on outer walls and yellow arrow shows the surface linking of nanotubes. Scale bars are in 50 nanometers. (For interpretation of the references to color in this figure legend, the reader is referred to the web version of the article.)

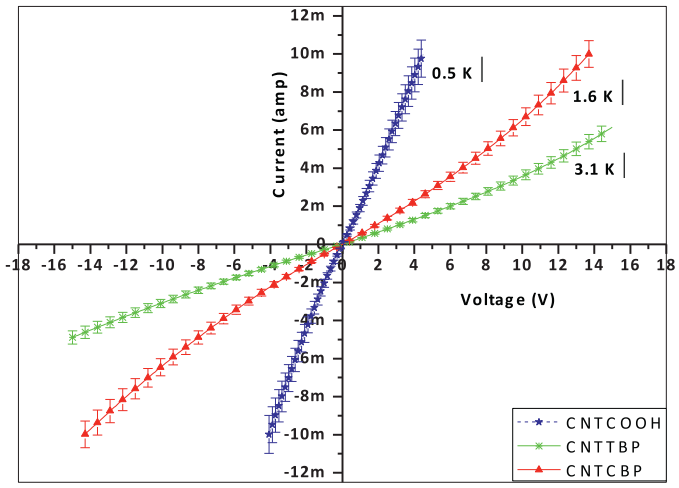

Fig. 6. *I–V* characteristic curves showing semimetallic behavior due to presence of semiconducting and metallic multiwall nanotubes in functionalized multiwall carbon nanotubes.

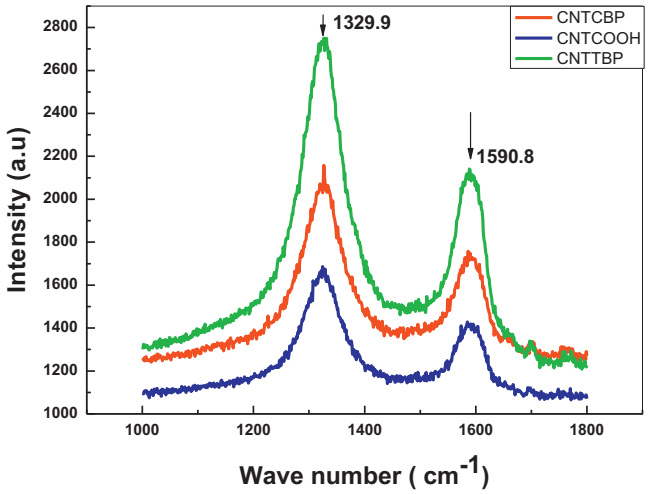

Fig. 7. Raman spectra of functionalized nanotubes and buckypapers.

of carboxylated buckypapers (CNTCBPs) from bottom to top (CNT to cross-linker ratio – 1:5, 1:7, 1:11) was 1.24%, 1.54% and 3.4% and response time 1.29 s, 3.7 s, 7 s and 6.05 s, respectively (Fig. 8a). Furthermore the sensitivity of thiolated buckypapers (CNTTBPs) from bottom to top was 3.36%, 3.8%, 8.87% and 16.07% and response time 6.09 s, 7.49 s, 11.59 s and 6.24 s, respectively (Fig. 8b).

The overall decrease in resistance of device was due to environmental effects and it can be reduced by operating the device under vacuum [35]. We observed that by increasing the CNTs to cross-linker ratio up to 1:9, results in increasing the sensitivity and response time of the device. Further increase in cross-linker makes the buckypaper brittle thus reduced sensitivity and the response time. Below this ratio (1:5) no buckypaper was formed. In case of CNTTBPs samples, we observed larger resistance change as compare to CNTCBPs samples on infrared illumination. We also observed the change in electrical properties after functionalization and small current flows through these devices. When carbon nanotubes were treated for thiolation and buckypaper formation, more defects along side walls were created as observed in Raman analysis. These defects causes down shift the Fermi level to the valance band [36] and may minimize the excitation of electrons under illumination which causes the resistance of the device to be increased as observed in electrical properties and infrared sensing of CNTTBPs samples.

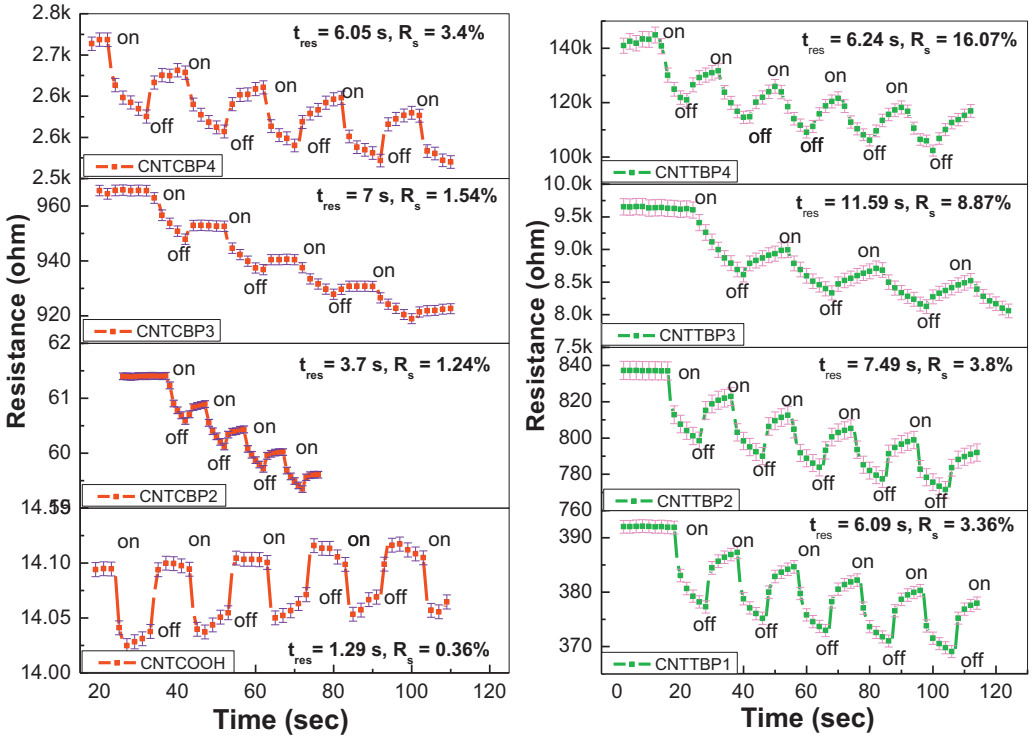

Fig. 8. Infrared sensor response of different prototypes of (a) CNTCOOH, CNTCBPs and (b) CNTTBPs.

4. Conclusions

We have successfully fabricated the infrared sensor device using functionalized multiwall carbon nanotubes buckypapers by varying the cross-linker reagent ratio in the buckypapers. The carbon nanotubes were functionalized by carboxyl and thiol group. FT-IR and Raman spectroscopic analysis confirmed the attachment of the functional groups. SEM analysis showed the morphology and agglomeration of nanotubes in the buckypapers. TEM analysis showed the outer wall defects produced by chemical treatments on carbon nanotubes. The MWCNT–COOH has smaller resistance (0.5 kΩ) then carboxylic and thiolated nanotubes buckypapers. CNTTBPs have large resistance (3.1 kΩ) so very small current flows as compare to CNTCBPs which have resistance of 1.6 kΩ. The cause of increase in resistance in buckypapers was due to increase in cross-linker reagent ratio in nanotubes. This increase in resistance of sensing material was verified by infrared sensing of buckypapers. The infrared sensor of thiolated buckypaper showed greater sensitivity response as compare to carboxylated buckypaper.

Acknowledgements

The authors are grateful to Prof. Fei WEI, Department of Chemical Engineering, Tsinghua University for characterization tools HRTEM, FESEM, FT-IR, Raman spectroscopy and electrical measurements unit FS-70Z with keithley source meter. We are also thankful to Prof. Dr. Tajammul Hussain (Late) NCP and Higher Education Commission (HEC) Pakistan for the financial support through "National Research Program for Universities" and COMSATS Institute of Information Technology.

References

[1] B. Yakobson, P. Avouris, M. Dresselhaus, G. Dresselhaus, P. Avouris, Carbon nanotubes: synthesis, structure, properties, and applications, Topics in Applied Physics 80 (2001) 287–327.
[2] U. Coscia, G. Ambrosone, A. Ambrosio, M. Ambrosio, F. Bussolotti, V. Carillo, et al., Photoconductivity of multiwalled CNT deposited by CVD, Solid State Sciences 11 (2009) 1806–1809.
[3] M. El Khakani, V. Le Borgne, B. Aïssa, F. Rosei, C. Scilletta, E. Speiser, et al., Photocurrent generation in random networks of multiwall-carbon-nanotubes grown by an all-laser process, Applied Physics Letters 95 (2009), 083114-3.
[4] W.-H. Chiang, D.N. Futaba, M. Yumura, K. Hata, Growth control of single-walled, double-walled, and triple-walled carbon nanotube forests by *a priori* electrical resistance measurement of catalyst films, Carbon 49 (2011) 4368–4375.
[5] C.-M. Seah, S.-P. Chai, A.R. Mohamed, Synthesis of aligned carbon nanotubes, Carbon 49 (2011) 4613–4635.
[6] X. Devaux, S.Y. Tsareva, A. Kovalenko, E. Zharikov, E. McRae, Formation mechanism and morphology of large branched carbon nano-structures, Carbon 47 (2009) 1244–1250.
[7] C. Kuzuya, W. In-Hwang, S. Hirako, Y. Hishikawa, S. Motojima, Preparation, morphology, and growth mechanism of carbon nanocoils, Chemical Vapor Deposition 8 (2002) 57–62.
[8] A. Goldoni, L. Petaccia, S. Lizzit, R. Larciprete, Sensing gases with carbon nanotubes: a review of the actual situation, Journal of Physics: Condensed Matter 22 (2010) 13001–13008.
[9] A. Gohier, A. Dhar, L. Gorintin, P. Bondavalli, Y. Bonnassieux, C.S. Cojocaru, All-printed infrared sensor based on multiwalled carbon nanotubes, Applied Physics Letters 98 (2011), 063103-3.
[10] D. Zhang, X. Deng, Z. Ji, X. Shen, L. Dong, M. Wu, et al., Long-term hepatotoxicity of polyethylene-glycol functionalized multi-walled carbon nanotubes in mice, Nanotechnology 21 (2010) 175101.
[11] A. Gohier, J. Chancolon, P. Chenevier, D. Porterat, M. Mayne-L'Hermite, C. Reynaud, Optimized network of multi-walled carbon nanotubes for chemical sensing, Nanotechnology 22 (2011) 105501.
[12] R. Lu, J.J. Shi, F.J. Baca, J.Z. Wu, High performance multiwall carbon nanotube bolometers, Journal of Applied Physics 108 (2010), 084305–5.
[13] M.E. Itkis, F. Borondics, A. Yu, R.C. Haddon, Bolometric infrared photoresponse of suspended single-walled carbon nanotube films, Science 312 (2006) 413–416.
[14] F. Rao, X. Liu, T. Li, Y. Zhou, Y. Wang, The synthesis and fabrication of horizontally aligned single-walled carbon nanotubes suspended across wide trenches for infrared detecting application, Nanotechnology 20 (2009) 055501.
[15] R. Lu, Z. Li, G. Xu, J.Z. Wu, Suspending single-wall carbon nanotube thin film infrared bolometers on microchannels, Applied Physics Letters 94 (2009) 163110–163113.
[16] Q. Zeng, S. Wang, L. Yang, Z. Wang, T. Pei, Z. Zhang, et al., Carbon nanotube arrays based high-performance infrared photodetector [Invited], Optical Materials Express 2 (2012) 839–848.
[17] J.-W. Zha, K. Shehzad, W.-K. Li, Z.-M. Dang, The effect of aspect ratio on the piezoresistive behavior of the multiwalled carbon nanotubes/thermoplastic elastomer nanocomposites, Journal of Applied Physics 113 (2013) 014102–14107.
[18] G. Vera-Reveles, T.J. Simmons, M. Bravo-Sánchez, M. Vidal, H. Navarro-Contreras, F.J. González, High-sensitivity bolometers from self-oriented single-walled carbon nanotube composites, ACS Applied Materials & Interfaces 3 (2011) 3200–3204.
[19] A.Y. Glamazda, V. Karachevtsev, W.B. Euler, I.A. Levitsky, Achieving high mid-IR bolometric responsivity for anisotropic composite materials from carbon nanotubes and polymers, Advanced Functional Materials 22 (2012) 2177–2186.
[20] M. Mahjouri-Samani, Y. Zhou, X. He, W. Xiong, P. Hilger, Y. Lu, Plasmonic-enhanced carbon nanotube infrared bolometers, Nanotechnology 24 (2013) 035502.
[21] B. Pradhan, K. Setyowati, H. Liu, D.H. Waldeck, J. Chen, Carbon nanotube-polymer nanocomposite infrared sensor, Nano Letters 8 (2008) 1142–1146.
[22] D.N. Ventura, R.A. Stone, K.-S. Chen, H.H. Hariri, K.A. Riddle, T.J. Fellers, et al., Assembly of cross-linked multi-walled carbon nanotube mats, Carbon 48 (2010) 987–994.
[23] K. Balasubramanian, M. Burghard, Chemically functionalized carbon nanotubes, Small 1 (2005) 180–192.
[24] J. Zhao, H. Park, J. Han, J.P. Lu, Electronic properties of carbon nanotubes with covalent sidewall functionalization, The Journal of Physical Chemistry B 108 (2004) 4227–4230.
[25] E. Gracia-Espino, G. Sala, F. Pino, N. Halonen, J. Luomahaara, J. Mäklin, et al., Electrical transport and field-effect transistors using inkjet-printed SWCNT films having different functional side groups, ACS Nano 4 (2010) 3318–3324.
[26] H. Park, J. Zhao, J.P. Lu, Effects of sidewall functionalization on conducting properties of single wall carbon nanotubes, Nano Letters 6 (2006) 916–919.
[27] M. Holzinger, O. Vostrowsky, A. Hirsch, F. Hennrich, M. Kappes, R. Weiss, et al., Sidewall functionalization of carbon nanotubes, Angewandte Chemie International Edition 40 (2001) 4002–4005.
[28] J.B. Lambert, H.F. Shurvell, R.G. Cooks, Introduction to Organic Spectroscopy, Macmillan, New York, 1987.
[29] D.L. Pavia, Introduction to spectroscopy: CengageBrain.com, 2009.
[30] X. Zhang, J. Liu, B. Xu, Y. Su, Y. Luo, Ultralight conducting polymer/carbon nanotube composite aerogels, Carbon 49 (2011) 1884–1893.
[31] A. Ugawa, J. Hwang, H. Gommans, H. Tashiro, A. Rinzler, D. Tanner, Far-infrared to visible optical conductivity of single-wall carbon nanotubes, Current Applied Physics 1 (2001) 45–49.
[32] K. Sato, R. Saito, Y. Oyama, J. Jiang, L. Cançado, M. Pimenta, et al., D-band Raman intensity of graphitic materials as a function of laser energy and crystallite size, Chemical physics letters 427 (2006) 117–121.
[33] T.-Y. Chen, T.-L. Lin, C.-C. Chen, C.-M. Chen, C.-F. Chen, Improved catalytic performance of pt supported on multi-wall carbon nanotubes as cathode for direct methanol fuel cell applications prepared by dual-stepped surface thiolation processes, Journal of the Chinese Chemical Society 56 (2009) 1236.
[34] B. Pradhan, R.R. Kohlmeyer, K. Setyowati, H.A. Owen, J. Chen, Advanced carbon nanotube/polymer composite infrared sensors, Carbon 47 (2009) 1686–1692.
[35] R. Afrin, J. Khaliq, M. Islam, I.H. Gul, A.S. Bhatti, U. Manzoor, Synthesis of multiwalled carbon nanotube-based infrared radiation detector, Sensors and Actuators A: Physical (2012).
[36] M. Burghard, Electronic and vibrational properties of chemically modified single-wall carbon nanotubes, Surface Science Reports 58 (2005) 1–109.

Biographies

Mrs. R. Afrin is a PhD scholar (Physics, Micro and Optoelectronics) at COMSATS Institute of Information Technology, Islamabad, Pakistan. Her research topic is Fabrication and characterization of carbon nanostructures for infrared and chemical sensor.

Dr. N.A. Shah completed his PhD in Quaid-i-Azam University Islamabad, Pakistan. Currently he is an Associate Professor of Physics at Department of Physics, COMSATS Institute of Information Technology, Islamabad and Principal Investigator, HEC Pakistan. He is a material scientist and currently working on the thin films solar cells for renewable energies.

Mr. M. Abbas is a PhD scholar (Materials Science and Engineering) at the Department of physics, COMSATS. His research interest is nanostructures for sensing applications and nano solar cells.

M. Amin is a PhD scholar (Physics, Micro and Optoelectronics) at COMSATS Institute of Information Technology, Islamabad, Pakistan. His research topic is Oxide semiconductor Nanostructures for Chemical Sensors.

Prof. Dr. A.S. Bhatti completed his PhD in University of Cambridge, Cambridge, UK. At present he is a professor and a Dean, Faculty of Science at Department of Physics, COMSATS Institute of Information Technology, Islamabad. He is a semiconductor physicist by training and recently working in synthesis and application of nanostructures for sensor applications. He established state of the art device fabrication facilities in this institute.